Proceedings of ICRC 2001: 1441 © Copernicus Gesellschaft 2001

ICRC 2001

Penetrating cascade showers observed by the emulsion chamber at high mountains

M. Tamada

Faculty of Science and Engineering, Kinki University, Osaka 577-8502, Japan

Abstract. The penetrating characteristics of the cascade showers observed by emulsion chambers at high mountains are studied by comparing with those in the simulated events obtained by the full Monte Carlo calculations through the atmosphere and the detector. A study is made for the Chacaltaya two-storey chambers and also to the Pamir joint carbon chambers applying just the same procedure both in the experiments and simulations. Although each chamber has a different structure, we find, in both chambers, an excess of the number of penetrating showers over the expectations. It amounts to $\sim 26\%$ of the penetrating showers in the Chacaltaya chambers and $\sim 43\%$ in the Pamir joint chambers.

1 Introduction

The Chacaltaya and Pamir emulsion chamber experiments have shown that there exist unusual phenomena which are not yet observed in the present accelerator experiments from the detailed analysis of high energy cosmic-ray families (a bundle of electromagnetic particles and hadrons produced in the nuclear and electromagnetic cascade process in the atmosphere) (Baradzei et al., 1992). Those are called 'Centauro-species', multiple hadron production without association of π^0-mesons. It is also discussed that the nature of secondary particles is possibly different from that of ordinary hadrons in those unusual phenomena based on the frequent observation of strong penetrating showers which became rejuvenated after passing through the target layer. In the paper (Funayama and Tamada,1984; Tamada,2001) we discussed about unusual behaviour of cascade development of the high energy showers in high-energy cosmic-ray families observed by Chacaltaya two-storey chambers no.18 and no.19. We studied in detail how the shape of the transition curve on the spot darkness of the observed showers, which penetrate from the upper chamber down to the lower chamber, deviate from that of (e, γ)-induced showers and of hadron-induced ones, and how often we can observe such penetrating showers, comparing experimental data with simulated cascade showers induced by (e, γ)-particles and by local hadron-interaction in the chamber assuming proper energy spectrum and zenith angle distribution. In the experiment, we can study such penetrating nature using the showers observed in the events which have at least two penetrating showers, because an exact upper-lower correspondence is necessary to do the analysis and is possible only for those events. It is, however, not easy to estimate how the above selection of the events distort the average characteristics of the families and of penetrating showers. Here we perform full Monte-Carlo calculation of the atmospheric families throughout the atmosphere and the detector, and apply just the same procedure both to the experimental and simulational data in order to make possible a direct comparison between the two.

Correspondence to: M. Tamada (tamada@me2.kindai.ac.jp)

2 The structure of the two-storey chambers

Fig.1 shows the basic structure of the Chacaltaya two-storey chambers no.18 and no.19 and of Pamir joint chamber P3'. The Chacaltaya chamber no.19 (no.18) consists of the upper chamber of 6 (7) cmPb, the target layer of 23 cm carbon (petroleum pitch), wooden support of 5cm thick, the air gap of 158 cm height and the lower chamber of 8.4 (9.6) cmPb. Four (five) sensitive layers (N-type X-ray film and nuclear emulsion plate) are inserted in the upper chamber and eight (nine) sensitive layers in the lower chamber. The Pamir joint carbon chamber P3' consists of the upper chamber of 6cm Pb, the target layer of 60 cm carbon and the lower chamber of 5 cmPb. The sensitive layers (N-type X-ray films) are inserted under 4 and 6 cmPb in the upper chamber and under 3 and 5 cmPb in the lower chamber. The shower, a bundle of electrons, induced by (e, γ)-particles or hadron interaction in the chamber, produce a small dark spot on the developed X-ray films at several successive layers. These shower spots are visible by the naked-eyes. The darkness detection threshold of the shower spot, measured by a $200 \times 200 \mu\text{m}^2$ slit, is

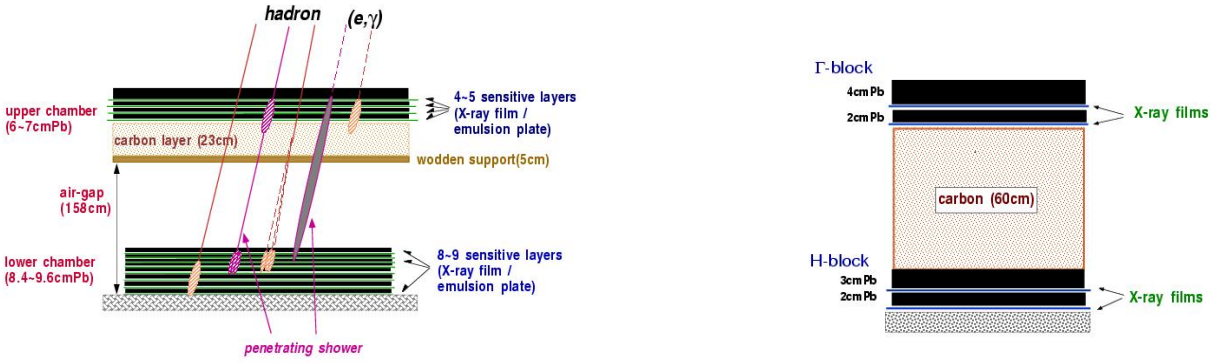

Fig. 1. Illustration of Chacaltaya two-storey chambers (left) and of Pamir joint chamber P3' (right).

around $D = 0.1$ for the N-type films.

3 Simulations of the atmospheric families

We use CORSIKA/QGSJET simulation code (Heck et al., 1998) for generating atmospheric families. 20,000 primaries of $E_0 \geq 10^{15}$ eV for the Chacaltaya chambers and 40,000 primaries for the Pamir chambers are sampled from the energy spectrum of 'normal chemical composition'. Nuclear and electromagnetic cascade in the atmosphere are followed until the energy of all the produced particles fall below 1 TeV or they arrive at the observation level. Zenith angle of the primary particles is selected at random in the interval between $0°$ and $45°$.

4 Detector simulation

For (e, γ)-particles and hadrons in the event, arriving upon the chamber, with total energy larger than 100 TeV, we calculate further nuclear and electromagnetic cascade development inside the chamber taking into account exactly the structure of each chamber.

4.1 Hadron-induced showers

We use QGSJET (Kalmykov et al.,1994) model for hadron-nucleus interactions, which is based on the Gribov-Regge theory of multiple Pomeron exchanges. In the nuclear cascade all hadrons, produced in the collisions during passage through the chamber, are followed until their energy falls below 80 GeV or they leave the chamber. The interaction mean free path of hadron-nucleus interactions is assumed to decrease with increasing interaction energy, e.g., $\Lambda_{p-Pb} = 15.9$ cm, $\Lambda_{\pi-Pb} = 17.5$ cm, $\Lambda_{K-Pb} = 18.0$ cm, $\Lambda_{p-C} = 56.1$ cm, $\Lambda_{\pi-C} = 71.3$ cm and $\Lambda_{K-C} = 78.5$ cm at $E = 10^{14}$eV. [1]

[1]For the Pamir chambers we take $\Lambda_{p-C} = 71.9$ cm, $\Lambda_{\pi-C} = 91.3$ cm and $\Lambda_{K-C} = 100.5$ cm at $E = 10^{14}$eV assuming the density of carbon layer is 1.0.

Since the shower-spot formation is mainly determined by high energy $\gamma-$rays, we further calculate the three-dimensional electromagnetic cascade development in the chamber for γ-rays of $E_\gamma \geq 1$ GeV, which are mainly decay products of π^0's produced in the collisions, using the Monte-Carlo code formulated by Okamoto and Shibata (1987), in which the LPM effect is also taken into account. Electrons and photons are followed until their energies fall below 1 MeV. Simulating electromagnetic cascade initiated by all the γ-rays of $E_\gamma \geq 1$TeV, we obtain the lateral distribution of the electron number density under every lead plate for the whole depth of the chamber. The electron number density, ρ_e, is converted to the local spot darkness, d, of X-ray film, by using the characteristic relation for the N-type X-ray film, [2] and finally we obtain the transition curve of the spot darkness D, measured by a $200 \times 200 \mu$m^2 slit, *vs.* depth T throughout the chamber. The experimental error of the measurement of spot darkness D is also taken into account by adding noise ΔD in each spot darkness where ΔD is sampled from Gaussian distribution with $\sigma_D = 0.1D$.

4.2 (e, γ)-induced showers

We also calculate electromagnetic cascade development in the chamber initiated by γ-rays and electrons in the events arriving upon the chamber, using the above mentioned Monte-Carlo code of electromagnetic cascade.

We thus obtain spot darkness throughout the chamber for all the member showers ((e, γ)- and hadron-origin) in the

[2]The sensitivity of X-ray films depends on the conditions of the exposure and development. Then it differs a little chamber by chamber. The calibration is carried out by track-counting method using accompanied nuclear emulsion plate. (In the Pamir joint chamber, we have several blocks, for the calibration, with sensitive layers composed of both X-ray films and nuclear emulsion plates.) Applying the calibration procedure in each chamber, it is found that the films have just a standard sensitivity in the chamber no.19, but they have 30 % more sensitivity in the chamber no.18 and 40 % less in the Pamir chamber P3'.

Table 1. Number of high energy showers in the atmospheric families of $100 \leq E_{tot} < 1,000$ TeV with more than two penetrating showers observed in the Chacaltaya chambers no.18, no.19 and Pamir chamber P3'.

	chamber no.18		chamber no.19		Pamir P3'	
	experiment	simulation	experiment	simulation	experiment	simulation
no. of events	10		12		49	
(a) showers observed only in the upper chamber (non-penetrating), $E(\gamma) \geq 10$TeV	42	38.4 ± 1.2 ($34.8\ e,\gamma$ / $3.6\ h$)	50	48.4 ± 1.5 ($44.0\ e,\gamma$ / $4.4\ h$)	232	238.3 ± 6.5 ($207.0\ e,\gamma$ / $31.3\ h$)
(b) showers observed only in the lower chamber, $E(\gamma) \geq 10$TeV	8	8.7 ± 0.5	7	7.3 ± 0.6	28	60.0 ± 3.2
(c) penetrating showers†	26	21.0 ± 0.9 ($11.9\ e,\gamma$ / $9.1\ h$)	41	28.3 ± 1.1 ($20.8\ e,\gamma$ / $7.5\ h$)	96	53.8 ± 3.1 ($41.4\ e,\gamma$ / $12.4\ h$)
(d) excess of penetrating showers over expectation	5 ± 5.2	12.7 ± 6.5 / 17.7 ± 8.3			42.2 ± 10.3	

Numerical values in the simulated events are normalized to the number of experimental events. Numerical values in the parenthesis are those of (e,γ)-induced and hadron-induced showers.
†) number of showers with $N_{upper}(D \geq 0.2) \geq 2$ and $N_{lower}(D \geq 0.2) \geq 1$ chosen irrespective of its energy.

family. The visible (detectable) energy of each shower is re-estimated by applying fitting procedure. That is, from a set of standard transition curves of $D^{std}vs.T$, calculated for showers of electron-positron pair origin taking into account the exact chamber structure, the best fit is selected by choosing the energy value, E, and the first pair-creation depth, ΔT, by a computer algorithm employing the gradient descent method for a search of the chi-square minimum.

5 Selection of the events

For the Chacaltaya chambers we selects events for the analysis which satisfy the following conditions;
1) the total visible energy, E_{tot}, is in the interval between 100 TeV and 1,000 TeV where minimum shower energy is taken to be 2 TeV and
2) the event has at least two penetrating showers in which the spot darkness at the bottom two layers in the upper chamber is larger than $D \geq 0.2$ and that at two successive layers in the lower chamber is larger than $D \geq 0.1$.

For the Pamir joint chamber we put the selection condition as;
1) E_{tot} is in the interval between 100 TeV and 1,000 TeV where minimum showers energy is taken to be 4 TeV and
2) the event has at least two penetrating showers in which the spot darkness of three layers among four sensitive layers at the experimental position is larger than $D \geq 0.1$.

The second condition is necessary to confirm the exact upper-lower correspondence. We observe 26 and 18 events with $100 \leq E_{tot} < 1,000$ TeV in one half of the Chacaltaya chamber no.18 and of no.19 respectively. 10 ($\sim$ 40%) among 26 events and 12 ($\sim$ 65 %) among 18 events satisfy the second selection criterion. In the Pamir joint chamber P3', we observe 91 events with $100 \leq E_{tot} < 1,000$ TeV. 49 ($\sim$ 55 %) events among them satisfy the second criterion. We apply just the same selection criteria also to the simulated events.

6 Penetrating cascade showers

In the events selected by the above two criteria some of the showers observed in the upper chamber can be followed down into the lower chamber. The observed high-energy showers are then classified into the following three categories.
(a) showers with visible energy $E(\gamma) \geq 10$ TeV observed only in the upper chamber (*non-penetrating showers*) defined as those which have no shower-spots of $D \geq 0.2$ in the lower chamber,
(b) those observed only in the lower chamber (C-jets, Pb-jets-lower) defined as showers which have no shower spots of $D \geq 0.1$ in the upper chamber and
(c) *penetrating showers*, irrespective of its energy, *re-defined* as a shower in which the spot darkness,D, is larger than 0.2 at least in two layers in the upper chamber, $N_{upper}(D \geq 0.2) \geq 2$, and at least in one layer in the lower chamber, $N_{lower}(D \geq 0.2) \geq 1$. A typical example of the transition curve of the penetrating shower is shown in Fig.2.

We summarise in Table 1 the number of showers of the three categories in the above selected events.

In order to demonstrate how the selection criterion (2) distort the average characteristics of the atmospheric families, we show in Table 2 the number of showers of the above three categories ((a), (b) and (c)) for the simulated events which satisfy the condition (1), i.e., events with $100 \leq E_{tot} < 1,000$ TeV, and those for the events which satisfy both criteria (1) and (2) respectively. As is seen in the table, the second criterion works in favour of more penetrating showers, $1.6 \sim 1.8$ times more than the average of all the events.

Table 2. Number of high energy showers per event in the simulated events.

	chamber no.18		chamber no.19		Pamir P3'	
selection criteria	(1) and (2) (290 events)	(1) (611 events)	(1) and (2) (269 events)	(1) (470 events)	(1) and (2) (277 events)	(1) (528 events)
(a)	3.84 ± 0.12 $\begin{pmatrix} 3.487\ e,\gamma \\ 0.36\ h \end{pmatrix}$	3.05 ± 0.07 $\begin{pmatrix} 2.77\ e,\gamma \\ 0.28\ h \end{pmatrix}$	4.03 ± 0.12 $\begin{pmatrix} 3.66\ e,\gamma \\ 0.37\ h \end{pmatrix}$	3.42 ± 0.09 $\begin{pmatrix} 3.12\ e,\gamma \\ 0.30\ h \end{pmatrix}$	4.86 ± 0.13 $\begin{pmatrix} 4.22\ e,\gamma \\ 0.64\ h \end{pmatrix}$	3.56 ± 0.08 $\begin{pmatrix} 3.11\ e,\gamma \\ 0.454\ h \end{pmatrix}$
(b)	0.87 ± 0.05	0.76 ± 0.04	0.61 ± 0.05	0.60 ± 0.04	1.22 ± 0.07	1.14 ± 0.05
(c)	2.10 ± 0.09 $\begin{pmatrix} 1.18\ e,\gamma \\ 0.92\ h \end{pmatrix}$	1.21 ± 0.05 $\begin{pmatrix} 0.64\ e,\gamma \\ 0.57\ h \end{pmatrix}$	2.36 ± 0.09 $\begin{pmatrix} 1.73\ e,\gamma \\ 0.63\ h \end{pmatrix}$	1.49 ± 0.06 $\begin{pmatrix} 1.08\ e,\gamma \\ 0.41\ h \end{pmatrix}$	1.10 ± 0.06 $\begin{pmatrix} 0.84\ e,\gamma \\ 0.25\ h \end{pmatrix}$	0.72 ± 0.04 $\begin{pmatrix} 0.53\ e,\gamma \\ 0.19\ h \end{pmatrix}$

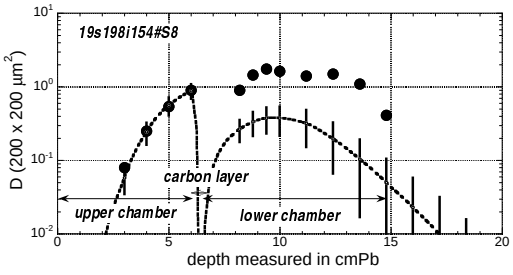

Fig. 2. An example of the transition curve on spot darkness of the penetrating showers observed in Chacaltaya chamber no.19. Dotted curve is an expected shower transition curve.

It is remarkable that the number of hadron-induced penetrating showers is almost same to that of showers in lower with $E(\gamma) \geq 10$ TeV in the Chacaltaya events. In Table 1 we show the number of showers of the three categories expected in the simulated events for the comparison with experimental data. Here the numerical values are normalized to the experimentally observed number of events in each chamber. We can see no considerable differences between simulations and experiments in the number of non-penetrating showers and showers in lower, except for the showers in lower in the Pamir chamber P3' where the simulational data gives ~ 2 times more than experimental value. For the penetrating showers, we can see around one half of the experimental penetrating showers can be explained by the (e,γ)-induced showers in all the three chambers. The other half of the penetrating showers then is expected to be hadron-induced ones, but it is seen that the number of those expected in the simulated events is much smaller than the observation, though the statistics is small in the Chacaltaya chambers. The raw (d) in the table gives the excess of the number of the penetrating showers over the expectation. It amounts to $\sim 26\%$ of the penetrating showers in the Chacaltaya chambers and $\sim 43\%$ in the Pamir joint chamber P3'.

7 Discussions

We have studied in detail the penetrating probability of showers in high energy atmospheric families observed by the Chacaltaya two-storey chambers and by the Pamir joint chambers. In order to make possible a direct comparison with experiment we carried out full Monte Carlo calculations of the atmospheric families throughout the atmosphere and the detector taking into account the exact structure of the chamber. The comparison shows that there exists a considerable excess of penetrating showers in the experiments over the expectation, accounting for $\sim$ 26 % of all the penetrating showers in the Chacaltaya chambers and $\sim$ 43 % in the Pamir joint chamber P3'. One of the possible explanations for the observed excess in the experiments is to assume the occurrence of extremely collimated pair of a γ-ray and a hadron. That is, if the mutual distance between a γ-ray and a hadron is extremely small, e.g., less than $\sim$ 1 mm, and the γ-ray-induced shower is observed in the upper chamber and the hadron-induced shower is observed in the lower chamber, we would possibly misidentify those two as a penetrating shower. If a γ-ray makes electromagnetic interactions in the atmosphere, we can observe collimated several (e,γ)-particles and a hadron as a 'mini-cluster' which are often found in the exotic events (Baradzei et al.,1992). Possible existence of hadron-bundles in which the mutual distance of the constituent hadrons is extremely small is also discussed in the analysis of transition curve of high-energy hadronic showers observed in the Pamir thick lead chamber (Tamada and Kopenkin,1997; Tamada and Ohsawa,2000).

Acknowledgements. This work is supported by Faculty of Science and Engineering of Kinki University, grant RK13-23.

References

Baradzei,L.T. et al.(Chacaltaya and Pamir collaboration), *Nucl. Phys. B* **370** (1992) 365
Funayama,Y. and Tamada,M., *J. Phys. Soc. Japan* **55**, (1986) 2977
Heck,D. et al., *FZKA report 6019, Forschungszentrum, GmbH Karlsruhe* 1998
Kalmykov,N.N., Ostapchenko,S.S., & Pavlov, A.I., *Bull. Russ. Acad. Sci. (physics)* **58** (1994) 1966
Okamoto,M and Shibata,T., *Nucl. Instr. Meth.* **A257** (1987) 155
Tamada,M. and Kopenkin,V.V., *Nucl. Phys. B* **494** (1997) 3
Tamada,M. and Ohsawa,A., *Nucl. Phys. B* **581** (2000) 73
Tamada,M., *Nucl. Phys. (Proc. Suupl.)* 97 (2001) 150